# Frontal increase of movement-related beta modulation is enhanced by visuo-motor learning

**Elisa Tatti** ( elisatatti86@gmail.com )
CUNY, School of Medicine
**Francesca Ferraioli**
CUNY, School of Medicine
**Jaime Peter**
CUNY, School of Medicine
**Tomi Alalade**
CUNY, School of Medicine
**Aaron Bruce Nelson**
CUNY, School of Medicine
**Serena Ricci**
CUNY, School of Medicine
**Angelo Quartarone**
Department of Biomedical, Dental Sciences and Morphological and Functional Images, University of Messina, Messina, Italy, 98125
**M. Felice Ghilardi**
CUNY, School of Medicine

**Research Article**

**Keywords:** EEG, ERD, ERS, post-movement beta synchronization, visuo-motor adaptation

**Posted Date:** March 11th, 2021

**DOI:** https://doi.org/10.21203/rs.3.rs-279532/v1

# Abstract

Recently we found that enhancements of movement-related beta (13.5–25 Hz) modulation (measured as event-related desynchronization peak to synchronization peak) during a simple reaching test (*mov*) occur over frontal and left sensorimotor regions after extended practice in a visuo-motor adaptation task (ROT) but not after similar duration practice in a visual learning task. Here we verify whether those enhancements are also trigged by motor practice alone or the additional learning component inherent in the visuo-motor adaptation task is needed. In healthy young subjects, beta modulation during *mov* increased over frontal and contralateral sensorimotor areas after three-hour practice of either ROT or reaching movements without visuo-motor adaptation (MOT). However, while the increase over the left area was similar after the two tasks, the frontal increase was greater after ROT practice.

These findings confirm previous reports that extensive practice leaves local traces in beta power both at rest and during the subsequent execution of a motor test. They further suggest that, since they occur after motor tasks with (ROT) and without learning (MOT), these traces likely express the cost of processes necessary both for usage of these areas and for the engagement of long-term potentiation mechanisms necessary for creating new internal models.


# Introduction

Movement is associated to modulation of beta oscillatory activity (13-25 Hz) over sensorimotor regions: movement preparation and execution are characterized by decreased beta power (event-related desynchronization, ERD), followed by a hefty rebound (event-related synchronization, ERS) once the movement is completed [1,2].

Over the last decades, several frameworks have been proposed to explain the functional role of sensorimotor beta power and its movement-related modulation [3–5]. At the present time, there is a general agreement in considering beta modulation as resulting from the interplay between motor and sensory regions. Accordingly, beta ERD should reflect the activation of the motor network and the increase in corticospinal excitability [6], while the subsequent rebound (ERS) would represent the activation of an extended network, which includes somatosensory and prefrontal regions, with the purpose of assessing and eventually update the activated motor representations. This updating process makes it likely that movement-related beta modulation, and ERS in particular, may be linked to the engagement of long-term potentiation- (LTP) and long-term depression (LTD)-mediated mechanisms. This hypothesis is in line with a series of recent reports; first, TMS studies have shown that facilitation of corticospinal excitability elicited with iTBS also results in increased beta ERS [7]. Second, EEG studies demonstrated a progressive enhancement of sensorimotor and frontal beta ERS amplitude with motor practice [8–11], learning [12] and sensorimotor adaptation [13]. Third, the practice-related increases of beta modulation depth (peak ERS-ERD) correlates with skill retention tested the following day [9] and led to local enhancements of beta power in the post-training resting state EEG [8,14], enhancements that vanish after both a period of quiet

rest and sleep [14]. Finally, in a recent study [15] we found that this carry-over effect was also present in movement-related beta modulation during an ensuing simple reaching test (*mov*). Indeed, after three one-hour motor learning in a task requiring implicit adaptation to a visually-rotated display (ROT), the increase of beta modulation during *mov* over frontal and contralateral sensorimotor regions was greater than after a visual learning task without motor component. This suggests that previous intensive motor learning locally enhances practice-related beta modulation increase.

Are the carry-over effects on beta modulation strictly related to motor learning or do they occur to the same degree after practice in a motor task without significant learning components? Recently [14], we have shown that ROT and MOT, a motor task with similar features as ROT but without rotation learning, share similar power changes in the beta range: in both, beta power increases over frontal and contralateral centro-parietal regions during the tasks and in the following resting state EEG. Would ROT and MOT tasks leave similar traces also in the movement-related beta modulation of a subsequent simple motor task?

As in our latest study [15], here we investigated whether extensive practice in MOT and extensive learning in ROT, would leave the same local traces on movement-related beta modulation during a successive simple planar reaching movement test (*mov*).

# Results

Two groups of healthy young subjects completed three morning sessions of intensive practice in one of two reaching tasks: ROT, where subjects constantly and implicitly adapted their movements to visual rotations of different degree or MOT, a control task kinematically equivalent to ROT but without important learning components. To determine the effects of task practice on general motor performance, at baseline and after the practice in the two tasks, both groups also completed a short block of *mov*, a simple reaching test with targets presented at three different distances.

*ROT and MOT practice differentially affect regional beta modulation amplitude*

To verify that the same degree of engagement was present across tasks and blocks, we first ascertained whether within-block changes of performance were similar in the first and last block of MOT and ROT. To allow for task comparisons unbiased from contamination of rotation learning, we focused on the kinematic data from the first and last 30 movements of MOT1, MOT3, ROT1 and ROT3. Indeed, all these trials were without imposed rotation also in ROT and, in case of the last movements, were performed after the after-effects of rotation mostly vanished. As the kinematic data in ROT and MOT were not normally distributed (see Methods), we used independent-samples Kruskal-Wallis and related-samples Wilcoxon-signed rank tests to assess between-tasks and between-blocks differences. Such comparisons revealed no significant changes both between tasks and between blocks for reaction time, movement time, and peak velocity (Supplemental Table S1), suggesting that the degree of engagement was similar.

We then asked whether, despite the similar engagement in terms of performance, the two types of practice left a specific hallmark in beta oscillatory activity. Therefore, we first focused on the changes of

mean beta power during tasks' performance and compared the differences between first and last sets of movements during the first block of both MOT (MOT1) and ROT (ROT1) with Bonferroni-corrected paired t-test permutation analyses (alpha = 0.01, see Methods). For both tasks, this analysis showed a considerable increase in the average beta power, with the greatest increment located over the frontal and left sensorimotor regions (significant electrodes, mean±SD: ROT1: 17.92±21.67%, t=3.44±0.67, p=0.002±0.002; MOT1: 14.91±12.31%, t=3.67±0.76, p=0.003; Figure 1a). During the third block (MOT3 and ROT3), the same analysis did not reveal any within-block increase in both tasks, suggesting a possible ceiling effect. Nevertheless, the same analyses with alpha threshold lowered at 0.05 revealed a significant within-block increase in a set of electrodes located over a similar left-frontal region both in ROT3 (6.18±12.44%, t=2.19±0.31, p=0.024±0.013) and MOT3, even though the enhancement was more localized in the prefrontal electrodes in the latter (7.77±10.71%, t=2.33±0.26, p=0.014). MOT3 presented also significant activity increase in electrodes over the right centro-parietal region (9.80±14.19%, t=2.22±0.26, p=0.025±0.009, Figure 1a). A direct comparison between the two tasks indicated that ROT and MOT displayed similar pattern of within-block beta power increase in both blocks. However, MOT3 showed a slightly larger increase in few electrodes over the left frontal (ROT3 vs MOT3: -7.9%, t=-1.96±0.15, p=0.026±0.012) and right parietal region in (ROT3 vs MOT3 vs: -9.45%, t=-1.98±0.16, p=0.029±0.09, Figure 1b).

We then determined whether the within-block changes (Last-First movements) of beta modulation depth amplitude (peak ERS-ERD) equally occurred in the first and last blocks. We focused these analyses on the three ROIs, i.e., Left, Right and Frontal, defined by the electrode with the maximum value of beta modulation depth and the six neighboring ones (see Methods). Due to violation of the normality assumption, we used a two-step non-parametric approach. In the first step, Wilcoxon Signed Rank tests were run separately for the two tasks and confirmed that, similarly to mean beta power, the within-block increase of beta modulation depth over the Left and Frontal ROIs was larger in the first compared to the third block for both ROT and MOT (Left ROI, ROT: z=-2.84, p=0.01; MOT: z=2.55, p=0.01; Frontal ROI, ROT: z=2.19, p=0.03; MOT: z=2.27, p=0.02) (Supplemental Table S2). These results are consistent with the findings regarding mean beta power and suggest that the within-block increase of beta power is maximal in the first block of both tasks with the possible presence of a ceiling effect in the last block.

In the second analysis step, we ascertained whether the observed beta modulation changes were similar in the two tasks. Independent-sample Kruskal-Wallis tests highlighted that, while in the first block the two tasks had comparable beta modulation growth in all the three ROIs, ROT3 showed greater increase than MOT3 in the Frontal ROI only (mean rank: ROT3=22.24, MOT3=14.23, H=4.442 p=0.035, Supplemental Table S2).

Altogether, these results indicate that in both ROT and MOT tasks within-block increases of beta power over frontal and parietal areas may follow a logarithmic trend, with a greater increase in the first block of practice and a lesser one in further training. Moreover, extensive practice of visuo-motor adaptation induces greater within-block increases of beta modulation over the frontal region, an increase that might reflect not only motor practice *per se*, but also learning-related processes.

*Simple motor practice and visuo-motor adaptation differentially affect frontal increase of beta modulation in a subsequent motor test*

We then compared *mov* tests, each composed by 96 movements presented at three distances and eight directions, performed at baseline (*mov*0) and after the third block (*mov*3) of both practiced tasks. *mov* tests were performed to determine whether, compared to MOT, the continuous visuomotor adaptation learning required by ROT led to performance deterioration and induced local changes in movement-related beta modulation during simple reaching movements.

Therefore, we first focused on the performance in both *mov*0 and *mov*3 and, in particular, on the number of correct numbers, defined as those movements with reaction time, normalized hand path area and directional error values falling within two SD of the baseline mean *mov*0. Using a mixed-model ANOVA because of the normal distribution, we found significant main effects of Block and Task with a significant Block X Task interaction (Table 1). Indeed, while performance levels in MOT*mov* and ROT*mov* were comparable at baseline (mean±SD, MOT*mov*0: 82.38%±8.33; ROT*mov*0: 81.81%±3.80, Table 1), after three blocks of ROT practice, the number of correct movements in *mov* significantly decreased (ROT*mov*3: 68.13%±10.09, MOT*mov*3: 86.35%±8.31; Table 1). The correct movements of all ROT*mov* and MOT*mov* had similar kinematic characteristics (Table 1). Altogether, these results support the hypothesis that the additional learning present in ROT but not in MOT might have induced more fatigue; this, in turn, might have led to performance deterioration, in agreement with previous results [14,15].

In the ROT task, beta modulation displayed greater increase over the frontal region compared to MOT. Thus, we next ascertained whether this was also the case during the ensuing *mov* test.

We first determined whether the average beta oscillatory activity increased in *mov* and whether such increase differed according to the practiced task. Non-parametric permutation analyses (alpha = 0.05) on the difference between *mov*3 and *mov*0 showed a strong increase of the average beta power for both ROT*mov* (mean±SD: 15.3%±21.0%, t= 2.52, p=0.009) and MOT*mov* (27.1%±21.0%; t= 2.40, p=0.02). Importantly, the direct comparison of ROT*mov* and MOT*mov* with independent-samples t-test permutation analysis showed greater power increase in ROT*mov* (mean±SD: 36.4%±52.3%) compared to MOT*mov* (1.6±25.0%; t= 1.74, p= 0.03) over frontal and right centroparietal regions (Figure 2).

We then explored the between-blocks (*mov*3 vs *mov*0) and between-groups (ROT*mov* vs MOT*mov*) differences in beta modulation, ERD and ERS amplitudes in the three ROIs (Left, Right and Frontal, see Methods). Again, because of the normality violation, a two-step non-parametric approach was adopted. In the first step, Wilcoxon Signed Ranks Tests were run to test practice-related changes (*mov*3-*mov*0) for each ROI and session (ROT*mov* and MOT*mov*). In agreement with a previous publication [15], in ROT*mov*, the amplitude of beta modulation and ERS significantly increased from *mov*0 to *mov*3 over the three ROIs, while beta ERD amplitude was reduced over the Right and Frontal ROIs. All these changes were accompanied by an increase of mean beta power in the three ROIs (Table 2). On the other hand, the same analyses on MOT*mov* revealed that the amplitude of beta modulation and ERS, as well as the beta

average power, increased only over the Left ROI (Table 2). These results indicate the occurrence of cumulative effect of practice in the subsequent reaching test; specifically, extended motor practice with negligible learning mostly affect beta activity over the left centro-parietal region whereas continuous visuo-motor adaptation, such as that taking place in ROT, is accompanied by an additional increase of beta modulation over the frontal region. Accordingly, these local changes in beta modulation depth might reflect use-dependent changes in the sensorimotor and frontal areas, with the first area similarly active in both tasks and the latter being more engaged during visuo-motor rotation.

We confirmed such difference between ROT*mov* and MOT*mov* in the second step, with a direct comparison of *mov*3-*mov*0 changes between the two groups by means of independent-sample Kruskal-Wallis tests. Compared to MOT*mov*, ROT*mov* showed greater practice-related changes for both beta modulation (H=5.46, p=0.019) and ERS (H=5.59, p=0.018) in the frontal ROI, and in the right ROI for the ERS only (H=4.02, p=0.045). No differences were observed between the two groups in the average beta power (Table 3).

Finally, we applied the *beamformer* DICS technique to estimate the sources responsible of the observed practice-related beta modulation changes between ROT*mov* and MOT*mov*. Non-parametric permutation test with Bonferroni correction was run to compare beta amplitude changes (*mov*3-*mov*0) between ROT*mov* and MOT*mov* sources. Importantly, as the channel-related results suggested that beta modulation depth changes were largely dependent from the increased ERS, source reconstruction focused on the post movement time window only (from 700-2000 ms, see Methods). Based on the human Brainnetome atlas parcellation, ROT*mov* was associated with greater post-movement beta increase in the right precentral (i.e., primary motor cortex) and right postcentral gyrus (i.e., primary somatosensory area), right medial and dorsolateral superior frontal gyrus, right middle frontal gyrus and middle cingulate gyrus bilaterally (Figure 3, Table 4). Interestingly, these areas are involved in the processes related in visuo-motor adaptation, as shown by previous imaging studies [16,17].

# Discussion

The present study shows that extended motor practice, independently of the learning load, leaves traces in movement-related beta modulation of a subsequent simple reaching task, albeit with topographies and magnitudes that reflect the differential engagement of the examined ROIs in the specific tasks. Also, the finding of a greater beta modulation increase over the frontal area after the visuo-motor learning task suggests that such traces may result from the combined footprint of motor practice *per se*, a characteristic common to the two tasks, and of the learning-related processes, which mostly occur during visuo-motor adaptation. Altogether, these findings support the hypothesis that the traces the task left on beta modulation in the following motor test may express phenomena related to the local “usage”, as discussed in the following paragraphs.

Beta modulation increases were present in *mov*, a simple reaching test, not only after extensive practice in a visuo-motor adaptation task, ROT, as in previous work [15], but also after practice in a motor task, MOT,

without relevant learning components. However, these increases differed in terms of local magnitude: significant enhancement of beta modulation occurred over all three ROIs after ROT, but only over the Left ROI after MOT. Therefore, such increases of beta modulation could be considered as traces of two tasks' activity in the ensuing *mov*. Indeed, these task-related differences already emerged during the ROT and MOT practice: while the degree of within-block increase over the three ROIs was similar during ROT1 and MOT1 tasks, beta modulation in the last block increased only over the frontal region during ROT3 and such an increase was greater than the corresponding one in MOT3. Importantly, these patterns of increase were mostly related to changes in beta ERS. The source reconstruction revealed that the estimated sources of the observed frontal ERS increase in ROT*mov*3 were localized in the right primary sensorimotor cortices, the pre-supplemental area and the middle region of the cingulate cortex. These sources are compatible with the findings of other studies on the distribution of ERS with neuroimaging and intracranial EEG recordings [18–21]. Beta ERS recorded over the frontal region has been associated to several functions supporting motor learning, such as the maintenance of sensorimotor representations [13,22–26], processing of sensory reafference [27,28] and visuomotor attention [3,29]. In particular, the frontal region is highly engaged during motor adaptation to visual rotations and the superior frontal gyrus, which likely corresponds to the pre-supplementary motor area, is specifically active in the earliest phases of exposure to visuo-motor rotation [17,30,31]. Indeed, our subjects were intentionally kept in the earliest stages of adaptation, with a new visual rotation introduced every two sets of movements. Finally, our sources indicated that ROT*mov* has a greater engagement of the right fronto-parietal regions, in line with their role in visual attention [32] and previous findings implicating the right hemisphere in visuo-motor adaptation [16,17,33,34]. Therefore, it is possible that, compared to the negligible learning load in MOT, the constantly greater engagement of these regions for visuo-motor adaptation might have led to greater neuronal activity in the frontal and right regions. It is not clear whether or not this greater neuronal activity is directly related to learning and plasticity-related phenomena.

A recent fMRI study by Bédard and Sanes [30] showed that while visuo-motor adaptation learning was associated with greater activity in the cerebellum, parietal and frontal areas, the activity of the right superior frontal gyrus was the only one not correlated with the magnitude of the after-effect.

The hypothesis that beta modulation increases over the frontal region might reflect neuronal processes not strictly related to learning is also supported by the fact that frontal beta modulation increase after the visuo-motor adaptation practice was not paralleled by specific improvement in the task performance [14] and that the carry-over effect in the subsequent test was accompanied by performance deterioration. This suggests that the practice-related beta modulation and ERS increases may reflect the local build-up of neuronal fatigue due to intensive local activity with increased neuronal firing usually accompanied by depletion of metabolic resources and persistent changes in ionic concentrations.

Support to this possibility comes from experimental evidence in humans and animals. Studies in humans have shown that, while sleep is needed to consolidate performance and to return practice-related local

theta power increases to baseline levels [14], a period of quiet rest is sufficient to restore practice-related beta power increases at rest [14] and also of movement-related beta modulation [15].

In addition, studies in rodents have shown that increases of beta power in both frontal and somatosensory areas during active wake occur in parallel with local increases, in the same areas, of lactate concentration, an integrative measure of energy consumption [35]. Indeed, *ex-vivo* slice studies directly linked lactate-concentration to the disruption the neuronal excitation-inhibition balance, specifically by reducing gamma-band rhythm due to transient ATP-shortage in fast-spiking inhibitory interneurons [36]. Interestingly, sharp wave-ripples, lower-energy expenditure oscillations characterizing waking immobility and slow-wave sleep, were not perturbed by lactate injection [37].

Therefore, it is possible that the local increases of beta ERS and movement-related modulation due to extensive motor practice may reflect the rise of energy consumption that is needed, in both MOT and ROT, for the buildup of neuronal firing activity and, in ROT, for the additional induction of early phases of LTP processes. In line with this, it would be interesting to assess the effects of extensive motor practice on brain lactate and GABA concentration by proton magnetic resonance spectroscopy (MRS).

In conclusion, our study confirms previous evidence that that extended motor practice leaves traces in the movement-related beta modulation of a subsequent simple motor test. Compared to motor practice with negligible learning requirement, continuous motor adaptation to novel visual rotations is associated with greater beta modulation depth increase over the frontal regions, an increase that is carried over on subsequent simple reaching movements. The observed effect might reflect local neuronal use-dependent processes. These processes are likely linked to energy consumption needed for neuronal firing and for the induction of LTP processes to create new motor representations. The saturation of beta modulation increase might thus represent a state of reduced energy availability and, in a second instance, a decreased capacity for plasticity.

# Methods

*Participants*

Two groups of subjects were recruited for this study: 28 participants (mean±SD: 24.38±3.96 years, 16 women) completed the ROT task session and 14 subjects (mean±SD: 24.99±5.43 years, 10 women) participated to the MOT task session (see below). Data from part of these subjects were presented in previous publication [15,38].

All subjects were right-handed, had normal or corrected vision and no history of disorders affecting the nervous system. The study was approved by the CUNY University Integrated Institutional Review Board (UI-IRB) and registered with the US Department of Health and Human Services Office for Human Research Protections. The experiment was performed in accordance with the ethical principles of the Declaration of

Helsinki and its subsequent amendments. Each participant signed an IRB-approved informed consent form before completing the experiment.

### Experimental design

Participants were comfortably seated in a sound-shielded room in front of a computer display and fitted with a 256-channel EEG Geodesic Sensor Net (Electrical Geodesics Inc., Eugene, OR).

Both the ROT and MOT groups underwent a baseline assessment (*mov*0) before and after (*mov*3) completing either three one-hour blocks of ROT, an implicit motor learning task, or MOT, a control task with the same features of ROT but with negligible learning components.

### Tasks and test

**The testing apparatus and the instructions to the subjects were the same for the two tasks (ROT and MOT) and the test (*mov*) and are detailed in previous publications [14,15,39]. Briefly, in all tasks and test, subjects performed out-and-back movements on a digitizing tablet starting from a central starting point to a target presented from 400 ms as a blackening circle on a screen placed in front of the subjects. Instructions were to move after the target presentation, as soon and fast as possible, without corrections and to reverse direction within the target circle without stopping. The cursor position on the screen and the central starting point were always visible. Target presentation was random in all tasks and test.**

**The tasks and the test differed in the following characteristics: i) the time interval between two target presentations was 3 s in the test and 1.5 s in the two tasks; ii) in the *mov* test, the targets were presented at three distances (4, 7 and 10 cm) in eight directions (45° separation) with their radius varying with their distance from the center (0.5 cm, 0.88 cm, 1.25 cm, respectively). A total of 96 targets were presented in each *mov* test.**

**In the two tasks, ROT and MOT, the target array consisted of eight, radially arranged, empty circles, all at 4 cm from a center point. In order to probe implicit learning processes, in ROT the direction of the**

**cursor on the screen was rotated relative to the direction of the hand on the tablet in steps of 10°, 20° or 30° each, either clockwise or counterclockwise, starting from 0° (no rotation) up to a maximum of 60°. For each block, we run 21 sets for ROT and 20 sets for MOT of 56 reaching movements with 30 s inter-set interval. Crucially, all three ROT blocks ended with 112 movements without rotations to avoid carry-over effects on the subsequent *mov* test. In the MOT task all the sets had no imposed rotation.**

### Kinematic data recording and analyses

The (x,y) coordinates of each movement's trajectory were recorded with a custom-designed software by E.T.T. s.r.l., MotorTaskManager, Genoa, Italy (http://www.ettsolutions.com) and analyzed using an ad-hoc Matlab-based pipeline. First, we filtered the coordinates with a Butterworth filter and then computed the first, second and third derivative of the trajectory to obtain velocity, acceleration and jerk for all the movements.

Following previous publications [16,31], several measures were computed for each movement; in this study we focused on: reaction time (time from target appearance to movement onset), movement time (duration of the outgoing movement), and amplitude of peak velocity.

Movements with kinematic measures outside two SD and those rejected from EEG preprocessing were excluded from further analyses. Importantly, to allow for a proper task comparison unbiased by the rotation learning occurring in the ROT task, only the movements with zero-degree imposed rotation were included in the behavioral performance analyses. Therefore, for both the ROT and MOT tasks, we extracted the kinematic characteristics of the first and last 30 movements of each block (ROT1, ROT3, MOT1, MOT3).

## EEG Recording and preprocessing

High density (HD) EEG data were acquired using a 256-channel HydroCel Geodesic Sensor Net (Electrical Geodesic Inc.) with a Net Amp 300 amplifier (250 Hz sampling rate, online reference electrode: Cz) and Net Station version 5.0 software. Impedances were kept below 50 kΩ throughout the recording to preserve a good signal-to-noise ratio. The entire preprocessing was carried out using the public Matlab toolbox EEGLAB version 13.6.5b [40,41]. The EEG continuous signal was FIR filtered between 1 and 80 Hz and Notch filtered at 60 Hz (59-61 Hz).

Recordings were then segmented in 4-s epochs centered on target onset, resulting in a total of 96 epochs for *mov*, and 1176 epochs for ROT and 1120 MOT tasks. A manual visual inspection of the data was carried out to remove epochs and channels containing sporadic artifacts. After trial rejection, the average

number of trials per subject was 70.09 ±18.93 and 77.75±13.50 for ROT*mov* and MOT*mov*, respectively. For the ROT and MOT tasks, we kept an average of 1001.24±93.28 epochs for ROT and 941.38±87.52 epochs for MOT.

Independent Component Analysis (ICA) with Principal Component Analysis (PCA)-based dimension reduction (max 108 components) was applied to remove stereotypical artifacts (e.g., eye blinks, heartbeat, and muscular activity).

We retained an average of 16.26±6.91 and 13.50±3.17 components for the ROT*mov* and MOT*mov* recordings, and 16.22±6.25 and 19.46±7.24 components for the ROT and MOT tasks, respectively.

Electrodes rejected due to artifacts or poor signal quality were reconstructed using spherical spline interpolation, whereas those located on the cheeks and neck were removed from later analysis, resulting in 180 electrodes. Finally, the signal was re-referenced to common average.

For the purposes of our investigation, we focused our analyses on the first and last blocks for both the test (*mov*0 and *mov*3) and the tasks (ROT/MOT1 and ROT/MOT3). All the subsequent analyses were carried out using the MATLAB Toolbox Fieldtrip [42].

## EEG data analyses

In order to avoid confounding effects from mis-executed movements, after the preprocessing we discarded epochs representing movements whose kinematic parameters exceeded two SD and time-locked the remaining trials to movement onset (-1 to 2.5 s).

For both tasks (ROT and MOT) and test (ROT*mov* and MOT*mov*) the signal was decomposed into their time-frequency representations by convolving the signal with complex Morlet Wavelets at linearly spaced frequencies (1-55 Hz, 0.5 Hz bins) and increasing number of cycles (3 to 10 cycles).

In the analyses of ROT and MOT tasks, we first explored whether the practice-related within-block changes in beta oscillatory activity (13.5 25 Hz) would differ between the two blocks and between the two tasks. To avoid the confounding effects of the imposed-rotation that was implemented in ROT, only the trials corresponding to zero-degree rotation were included. Thus, for both the ROT and MOT tasks, the within-block increase is represented by the difference between the last and first two zero-degree sets of each block (ROT1, MOT1, ROT3, MOT3). Importantly, for each block, the first and last trials were normalized by subtracting and dividing the average signal of the entire time-window of all trials.

As the *mov* test was implemented to assess the spectral changes occurring after extensive ROT or MOT practice, the signal was normalized by subtracting and dividing each trial by the average signal of all the trials in the entire time-window of the baseline test (*mov*0).

Because their average beta power was exceeding 2 SD of the group average we removed: three subjects from ROT, one subject from MOT and one subject from ROT*mov*. Thus, the resulting sample size was 25

and 13 subjects for the ROT and MOT tasks, and 27 and 14 subjects for ROT*mov* and MOT*mov*, respectively.

## Statistical analysis

*Beta power analysis*

For the ROT and MOT tasks and their respective *mov* tests (ROT*mov* and MOT*mov*), analyses on practice-related changes in average beta power were conducted with Bonferroni-corrected Monte Carlo non-parametric permutation statistics (10000 permutations).

Non-parametric paired t-test permutation analysis on the between-blocks changes in practice-related beta power increase ($Block1_{last-first}$ vs $Block3_{last-first}$) were first run on the two tasks separately. The alpha threshold was set at 0.01 for the first block (ROT1 and MOT1) and, due to lack of statistically significant results with alpha=0.01, at 0.05 for the third block (ROT3 and MOT3). Further, in order to unveil possible differences in the practice-related beta power increase in the two tasks, independent-samples t-test permutation analyses were run to compare Block1 (ROT1 and MOT1) and Block3 (ROT3 and MOT3) practice-related changes in the two groups (alpha=0.05).

For the ensuing *mov* tests (ROT*mov* and MOT*mov*), the same approach was followed. Paired t-test permutation analyses (alpha = 0.05) were run to characterize between-block changes (*mov*0 vs *mov*3) in beta oscillatory activity in the two groups separately. These analyses were followed by an unpaired t-test statistic to directly assess differences in practice-related beta power changes between the two groups (ROT*mov*0-ROT*mov*3 vs MOT*mov*0-MOT*mov*3, alpha=0.05).

## Beta modulation analysis

Following our previous publications [15,39], movement-related beta modulation analyses were conducted using a personalized approach.

For each participant, we run time-frequency representations within the beta frequency range (13.5-25 Hz) using Complex Morlet Wavelets at linearly spaced frequencies (0.5 Hz bins, 10 cycles) on *mov*0, normalizing the signal by the average of beta power over the entire epoch. Next, the beta ERD and ERS peak amplitude and timing were computed over three broad regions corresponding to electrodes located on the frontal, left, and right sections of the EEG net. Peak ERD was defined as the minimum value of beta power between 100 ms before movement onset to 950 ms after, whereas the peak ERS was the maximum value in the 700 to 2500 ms time range. The beta ERS-ERD peak-to-peak difference (beta modulation depth) was consequently computed for each broad region to identify the electrode with the maximum beta modulation depth and the six neighbor ones. Throughout the paper, these electrode selections are denoted as Frontal, Left, and Right Regions of Interest (ROIs). The same procedure was carried out for both ROT1 and MOT1 with the following time intervals: -200 to 700 ms for the peak ERD and 500 to 1200 ms for the peak ERS.

For both the *mov* test and ROT/MOT tasks, time-frequency analyses were carried out on the selected ROIs (1:55 Hz, 0.5 Hz bins, 3:10 wavelet cycles) and normalized by subtracting and dividing by the average power over the entire time-window for all the trials. Peak beta ERS, ERD, modulation depth magnitude, as well as the ERS and ERD peak timing values were finally extracted for subsequent statistical analysis.

### Kinematics and *mov* EEG indices

In order to ascertain whether a parametric test was the appropriate statistical tool to test our data, both Shapiro–Wilks tests and Kolmogorov–Smirnov tests were run on the standardized residuals of the behavioral and EEG analyses to check for normality.

As no violation was observed for all the behavioral indices, mixed-model ANOVAs (with Blocks as within-subjects factor and Group as between-subjects factor) were run to test for any practice effect on *mov* kinematics.

For what concerns the EEG indices (peak beta ERS and ERD amplitude, beta modulation depth), as normality assumption was violated ($p < 0.05$), Wilcoxon Signed Ranks Tests were first run on ROT*mov* and MOT*mov* separately to check for blocks differences in each ROI (*mov*3 vs *mov*0). Between-groups differences were assessed for each ROI on the difference between *mov*0 and *mov*3 (*mov*3- *mov*0) with Kruskal-Wallis Tests.

### Source analysis

To identify the source responsible for the observed practice-related power changes, we also estimated the sources of beta oscillatory activity during a broad post-movement time window (0.7-2 s), where the beta ERS typically occurs.

For this purpose, we applied a beamforming approach, the Dynamical Imaging of Coherent Sources (DICS) method, and the estimates were calculated in the frequency domain [43].

We first computed the cross-spectral density (CSDs) matrices of the two blocks of interest (*mov*0 and *mov*3) using multitaper spectral estimates in the beta band (13.5-25 Hz) averaged over a broad beta ERS time window (0.7-2 s).

Since individual anatomical MRIs were not collected for this study, we applied a template volume conduction model of the head based on the boundary element method (BEM), a 3-compartment (scalp, skull and brain) model provided by Fieldftrip [42]. The BEM model and standard EEG electrode positions were co-registered by projecting all electrodes to the nearest point on the head surface mesh and computing a bilinear interpolation matrix from vertices to electrodes. The bioelectric forward problem was formulated as a leadfield matrix, where each column corresponds with the potential distribution on all channels for one of the x,y,z orientation of the dipole.

Source reconstruction was performed on each subject using a spatial filter computed on the combined *mov*0 and *mov*3 CSD matrices; the resulting source was then contrasted as follows: (*mov*3 – *mov*0)/*mov*0. Once each subject's source was reconstructed, the grand-averages of ROT*mov* and MOT*mov* sources were statistically compared to highlight whether the differences observed on the channel-level could also be observed at the source level.

Non-parametric Monte Carlo permutation test with Bonferroni correction (10000 permutations, alpha=0.05) was applied. To identify the corresponding MNI coordinates of the significant voxels, the statistic output was interpolated with the Brainnetome Atlas [44], a cross-validated atlas based on structural and functional connectivity measures.

# Declarations


### Acknowledgments

This work was supported by NIH P01 NS083514 (MFG). Kinematic data were collected with custom-designed software, MotorTaskManager, produced by E.T.T. s.r.l. We thank Martina Bossini Baroggi, Giulia Aurora Albanese and Giorgia Marchesi for the implementation of the kinematic analysis program (Marky) that was used to mark the kinematic data and Ramtin Mehraram for help in collecting and analyzing some of the MOT task data.


### Author Contributions Statement

Study conception and design: M.F.G., E.T., A.Q. Data acquisition: E.T., S.R., A.B.N. Data analyses: E.T., F.F., J.P., T.A., M.F.G. Interpretation of the results: E.T., F.F., A.Q., M.F.G. Manuscript drafting: E.T., F.F., M.F.G., A.Q. Manuscript revising: E.T., F.F., S.R., M.F.G., A.Q. All the authors agreed to be accountable for all aspects of the work in ensuring that questions related to the accuracy or integrity of any part of the work are appropriately investigated and resolved.

### Conflict of Interest Statement

The authors declare that the study was conducted in the absence of any commercial or financial relationships that could be construed as a potential conflict of interest.

# References


1. Lopes da Silva, F. H. & Pfurtscheller, G. Event-related EEG/MEG synchronization and desynchronization: basic principles. *Clin. Neurophysiol.***110**, 1842–1857 (1999).
2. Neuper, C., Wortz, M. & Pfurtscheller, G. ERD/ERS patterns reflecting sensorimotor activation and deactivation. *Prog. Brain Res.***159**, 211–222 (2006).
3. Kilavik, B. E., Zaepffel, M., Brovelli, A., MacKay, W. A. & Riehle, A. The ups and downs of beta oscillations in sensorimotor cortex. *Experimental Neurology***245**, 15–26 (2013).

4. Cao, L. & Hu, Y.-M. Beta Rebound in Visuomotor Adaptation: Still the Status Quo? *J. Neurosci.***36**, 6365–6367 (2016).
5. Spitzer, B. & Haegens, S. Beyond the status quo: A role for beta oscillations in endogenous content (RE)activation. *eNeuro***4**, (2017).
6. Chen, R., Yaseen, Z., Cohen, L. G. & Hallett, M. Time course of corticospinal excitability in reaction time and self-paced movements. *Ann. Neurol.***44**, 317–325 (1998).
7. Hsu, Y. F. *et al.* Intermittent theta burst stimulation over primary motor cortex enhances movement-related beta synchronisation. *Clin. Neurophysiol.***122**, 2260–2267 (2011).
8. Moisello, C. *et al.* Practice changes beta power at rest and its modulation during movement in healthy subjects but not in patients with Parkinson's disease. *Brain and Behavior***5**, (2015).
9. Nelson, A. B. *et al.* Beta Oscillatory Changes and Retention of Motor Skills during Practice in Healthy Subjects and in Patients with Parkinson's Disease. *Frontiers in Human Neuroscience***11**, (2017).
10. Tatti, E. *et al.* Beta modulation depth is not linked to movement features. *Front. Behav. Neurosci.***13**, (2019).
11. Ricci, S. *et al.* Aging does not affect beta modulation during reaching movements. *Neural Plast.***2019**, (2019).
12. Boonstra, T. W., Daffertshofer, A., Breakspear, M. & Beek, P. J. Multivariate time-frequency analysis of electromagnetic brain activity during bimanual motor learning. *Neuroimage***36**, 370–377 (2007).
13. Tan, H., Wade, C. & Brown, P. Post-Movement Beta Activity in Sensorimotor Cortex Indexes Confidence in the Estimations from Internal Models. *J. Neurosci.***36**, 1516–1528 (2016).
14. Nelson, A. B. *et al.* Neural fatigue due to intensive learning is reversed by a nap but not by quiet waking. *Sleep***44**, (2021).
15. Tatti, E. *et al.* Prior Practice Affects Movement-Related Beta Modulation and Quiet Wake Restores It to Baseline . *Frontiers in Systems Neuroscience* **14**, 61 (2020).
16. Ghilardi, M. *et al.* Patterns of regional brain activation associated with different forms of motor learning. *Brain Res.***871**, 127–145 (2000).
17. Krakauer, J. W. *et al.* Differential Cortical and Subcortical Activations in Learning Rotations and Gains for Reaching: A PET Study. *J. Neurophysiol.***91**, 924–933 (2004).
18. Crone, N. E. *et al.* Functional mapping of human sensorimotor cortex with electrocorticographic spectral analysis. I. Alpha and beta event-related desynchronization. *Brain***121 ( Pt 1**, 2271–2299 (1998).
19. Ohara, S. *et al.* Movement-related change of electrocorticographic activity in human supplementary motor area proper. *Brain***123 ( Pt 6**, 1203–1215 (2000).
20. Szurhaj, W. *et al.* Basic mechanisms of central rhythms reactivity to preparation and execution of a voluntary movement: a stereoelectroencephalographic study. *Clin. Neurophysiol.***114**, 107–119 (2003).

21. Parkes, L. M., Bastiaansen, M. C. M. & Norris, D. G. Combining EEG and fMRI to investigate the post-movement beta rebound. *Neuroimage***29**, 685–696 (2006).
22. Gilbertson, T. *et al.* Existing motor state is favored at the expense of new movement during 13-35 Hz oscillatory synchrony in the human corticospinal system. *J. Neurosci.***25**, 7771–7779 (2005).
23. Pogosyan, A., Gaynor, L. D., Eusebio, A. & Brown, P. Boosting cortical activity at Beta-band frequencies slows movement in humans. *Curr. Biol.***19**, 1637–1641 (2009).
24. Tan, H., Jenkinson, N. & Brown, P. Dynamic neural correlates of motor error monitoring and adaptation during trial-to-trial learning. *J. Neurosci.***34**, 5678–5688 (2014).
25. Tan, H. *et al.* Human subthalamic nucleus in movement error detection and its evaluation during visuomotor adaptation. *J. Neurosci.***34**, 16744–16754 (2014).
26. Engel, A. K. & Fries, P. Beta-band oscillations-signalling the status quo? *Current Opinion in Neurobiology***20**, 156–165 (2010).
27. Cassim, F. *et al.* Does post-movement beta synchronization reflect an idling motor cortex? *Neuroreport***12**, 3859–3863 (2001).
28. Alegre, M. *et al.* Beta electroencephalograph changes during passive movements: Sensory afferences contribute to beta event-related desynchronization in humans. *Neurosci. Lett.***331**, 29–32 (2002).
29. Classen, J., Gerloff, C., Honda, M. & Hallett, M. Integrative visuomotor behavior is associated with interregionally coherent oscillations in the human brain. *Journal of Neurophysiology***79**, 1567–1573 (1998).
30. Bédard, P. & Sanes, J. N. Brain representations for acquiring and recalling visual-motor adaptations. *Neuroimage***101**, 225–235 (2014).
31. Perfetti, B. *et al.* Modulation of gamma and theta spectral amplitude and phase synchronization is associated with the development of visuo-motor learning. *J. Neurosci.***31**, 14810–14819 (2011).
32. Bartolomeo, P. & Seidel Malkinson, T. Hemispheric lateralization of attention processes in the human brain. *Curr. Opin. Psychol.***29**, 90–96 (2019).
33. Huber, R., Ghilardi, M. F., Massimini, M. & Tononi, G. Local sleep and learning. *Nature***430**, 78–81 (2004).
34. Perfetti, B. *et al.* Modulation of Gamma and Theta Spectral Amplitude and Phase Synchronization Is Associated with the Development of Visuo-Motor Learning. *J. Neurosci.* (2011). doi:10.1523/JNEUROSCI.1319-11.2011
35. Grønli, J., Rempe, M. J., Clegern, W. C., Schmidt, M. & Wisor, J. P. Beta EEG reflects sensory processing in active wakefulness and homeostatic sleep drive in quiet wakefulness. *J. Sleep Res.***25**, 257–268 (2016).
36. Dienel, G. A. Brain Glucose Metabolism: Integration of Energetics with Function. *Physiol. Rev.***99**, 949–1045 (2019).
37. Hollnagel, J.-O. *et al.* Lactate Attenuates Synaptic Transmission and Affects Brain Rhythms Featuring High Energy Expenditure. *iScience***23**, 101316 (2020).

38. Nelson, A. B. *et al.* Neural fatigue due to intensive learning is reversed by a nap but not by quiet waking. *Sleep***44**, (2021).
39. Tatti, E. *et al.* Beta modulation depth is not linked to movement features. *Front. Behav. Neurosci.***13**, 1–6 (2019).
40. Delorme, A. & Makeig, S. EEGLAB: an open source toolbox for analysis of single-trial EEG dynamics including independent component analysis. *J. Neurosci. Methods***134**, 9–21 (2004).
41. Makeig, S., Debener, S., Onton, J. & Delorme, A. Mining event-related brain dynamics. *Trends Cogn. Sci.***8**, 204–210 (2004).
42. Oostenveld, R., Fries, P., Maris, E. & Schoffelen, J.-M. FieldTrip: Open source software for advanced analysis of MEG, EEG, and invasive electrophysiological data. *Comput. Intell. Neurosci.***2011**, 156869 (2011).
43. Gross, J. *et al.* Dynamic imaging of coherent sources: Studying neural interactions in the human brain. *Proc. Natl. Acad. Sci.***98**, 694 LP – 699 (2001).
44. Fan, L. *et al.* The Human Brainnetome Atlas: A New Brain Atlas Based on Connectional Architecture. *Cereb. Cortex***26**, 3508–3526 (2016).

# Tables

**Table 1.**

| | | Reaction Time *(ms)* | Peak Velocity *(cm/s)* | Movement Time *(ms)* | % Correct Movements |
|---|---|---|---|---|---|
| ROT*mov*0 | | 293.36± 27.92 | 57.31± 11.43 | 256.59± 46.54 | 81.81±3.80 |
| ROT*mov*3 | | 293.59± 28.04 | 57.53± 11.07 | 257.48±41.80 | 68.13±10.09 |
| MOT*mov*0 | | 303.40± 29.52 | 55.26± 11.04 | 281.30± 46.96 | 82.38± 8.33 |
| MOT*mov*3 | | 310.72± 28.72 | 52.93± 10.10 | 283.75± 49.39 | 86.35± 8.31 |
| Task df (1, 39) | F | 2.325 | 0.943 | 3.133 | 19.683 |
| | p | 0.135 | 0.337 | 0.085 | **< 0.001** |
| | $\eta^2_p$ | 0.056 | 0.024 | 0.074 | 0.335 |
| Block df (1, 39) | F | 1.803 | 0.740 | 0.154 | 10.615 |
| | p | 0.187 | 0.395 | 0.697 | **0.002** |
| | $\eta^2_p$ | 0.044 | 0.019 | 0.004 | 0.214 |
| Task * Bl df (1, 1) | F | 1.589 | 1.081 | 0.034 | 35.035 |
| | p | 0.215 | 0.305 | 0.856 | **< 0.001** |
| | $\eta^2_p$ | 0.039 | 0.027 | 0.001 | 0.473 |

able 1. *mov* performance indices. In the first four lines are reported the mean ± standard eviations (SD) for each *mov* test. In the following lines, the results of mixed-model ANOVAs

ascertaining the effects of block and preceding task on those indices are reported. Significant differences are reported in bold. F: test statistics; p: p values; $\eta^2_p$: Partial Eta Squared.

**Table 2**

| | | β ERD | | β ERS | | β modulation | | β mean power | |
|---|---|---|---|---|---|---|---|---|---|
| | | ROT *mov* | MOT *mov* | ROT *mov* | MOT *mov* | ROT *mov* | MOT *mov* | ROT *mov* | MOT *mov* |
| Left ROI | Z | 1.946 | 1.412 | 3.892 | 2.668 | 3.988 | 2.605 | 3.700 | 2.103 |
| | p | 0.052 | 0.158 | **0.002** | **0.008** | **0.002** | **0.009** | **0.002** | **0.035** |
| | $\tilde{\mu}$ 0 | -0.725 | -0.744 | 2.054 | 1.921 | 2.760 | 2.650 | 0.026 | 0.020 |
| | $\tilde{\mu}$ 3 | -0.705 | -0.731 | 3.061 | 3.159 | 3.690 | 3.875 | 0.245 | 0.397 |
| Right ROI | Z | 2.066 | 0.345 | 3.171 | 0.157 | 3.051 | 0.094 | 2.715 | 0.345 |
| | p | **0.039** | 0.730 | **0.002** | 0.875 | **0.002** | 0.925 | **0.007** | 0.730 |
| | $\tilde{\mu}$ 0 | -0.699 | -0.718 | 1.671 | 1.748 | 2.330 | 2.485 | 0.018 | 0.014 |
| | $\tilde{\mu}$ 3 | -0.684 | -0.724 | 1.970 | 1.567 | 2.640 | 2.305 | 0.109 | -0.005 |
| Front ROI | Z | 2.955 | -0.408 | 4.084 | 0.345 | 3.950 | 0.471 | 2.330 | 0.408 |
| | p | **0.003** | 0.683 | **0.002** | 0.730 | **0.002** | 0.638 | **0.020** | 0.683 |
| | $\tilde{\mu}$ 0 | -0.731 | -0.727 | 1.973 | 1.953 | 2.720 | 2.705 | 0.013 | 0.014 |
| | $\tilde{\mu}$ 3 | -0.686 | -0.764 | 2.918 | 1.768 | 3.600 | 2.525 | 0.094 | 0.024 |

**Table 2.** Comparison of beta ERD, ERS, modulation depth and mean power magnitude during the baseline (*mov*0) and third block (*mov*3) in ROT*mov* and MOT*mov*. Results of related-samples Wilcoxon Signed Rank Test on the differences between the two blocks (*mov*3 vs *mov*0) in each ROI and group (ROT*mov* and MOT*mov*). Z: test statistic; p: p values; $\tilde{\mu}$: median.

| | | β ERD | β ERS | β modulation | β mean power |
|---|---|---|---|---|---|
| Left ROI | H | 0.11 | 0.05 | 0.00 | 0.59 |
| | p | 0.74 | 0.83 | 1.00 | 0.44 |
| | μR ROT*mov* | 21.44 | 20.70 | 21.00 | 19.96 |
| | μR MOT*mov* | 20.14 | 21.57 | 21.00 | 23.00 |
| Right ROI | H | 0.98 | 4.03 | 3.19 | 2.12 |
| | p | 0.32 | **0.05** | 0.07 | 0.15 |
| | μR ROT*mov* | 22.33 | 23.70 | 23.41 | 22.96 |
| | μR MOT*mov* | 18.43 | 15.79 | 16.36 | 17.21 |
| Frontal ROI | H | 4.72 | 5.59 | 5.46 | 2.04 |
| | p | **0.03** | **0.02** | **0.02** | 0.15 |
| | μR ROT*mov* | 23.93 | 24.19 | 24.15 | 22.93 |
| | μR MOT*mov* | 15.36 | 14.86 | 14.93 | 17.29 |

**Table 4**

| Area | Brainnetome atlas label | voxels % | t (M) | t (SD) | p (M) | p (SD) |
|---|---|---|---|---|---|---|
| Superior Frontal Gyrus | R SFG, A8m | 91.42 | 1.85 | 0.17 | 0.03 | 0.01 |
| | L SFG, A8m | 87.05 | 1.69 | 0.08 | 0.04 | 0.01 |
| | R SFG, A6dl | 98.35 | 2.42 | 0.13 | 0.01 | 0.00 |
| | R SFG, A6m | 99.87 | 2.27 | 0.17 | 0.01 | 0.01 |
| | L SFG, A6m | 70.27 | 1.69 | 0.23 | 0.05 | 0.03 |
| Middle Frontal Gyrus | R MFG, A6vl | 98.57 | 2.14 | 0.23 | 0.01 | 0.01 |
| Precentral Gyrus | R PrG, A6cdl | 93.78 | 2.26 | 0.34 | 0.01 | 0.02 |
| | R PrG, A4ul | 99.80 | 2.31 | 0.19 | 0.01 | 0.01 |
| | R PrG, A4t | 96.95 | 2.10 | 0.23 | 0.02 | 0.01 |
| Paracentral Lobule | R PCL, A1/2/3ll | 91.71 | 1.75 | 0.13 | 0.04 | 0.01 |
| | R PCL, A4ll | 99.81 | 2.03 | 0.19 | 0.02 | 0.01 |
| | L PCL, A4ll | 73.16 | 1.71 | 0.15 | 0.04 | 0.02 |
| Postcentral Gyrus | R PoG, A1/2/3tru | 77.51 | 1.99 | 0.29 | 0.04 | 0.03 |
| Cingulate Gyrus | R CG, A24cd | 72.17 | 1.85 | 0.23 | 0.04 | 0.02 |
| | R CG, A23c | 100 | 2.11 | 0.20 | 0.02 | 0.01 |
| | L CG, A23c | 85.49 | 1.82 | 0.17 | 0.03 | 0.02 |

**Table 4.** Monte Carlo non-parametric permutation statistics on the difference between ROT*mov* and MOT*mov* between-blocks (*mov*3-*mov*0) post-movement beta power increase. Bonferroni correction was applied to address the multiple comparisons problem. Only significant sources according to the Brainnetome atlas are reported. Voxel % refers to the percentage of significant voxels for the corresponding area; M and SD are respectively the mean and standard deviation of t and p values.

# Figures

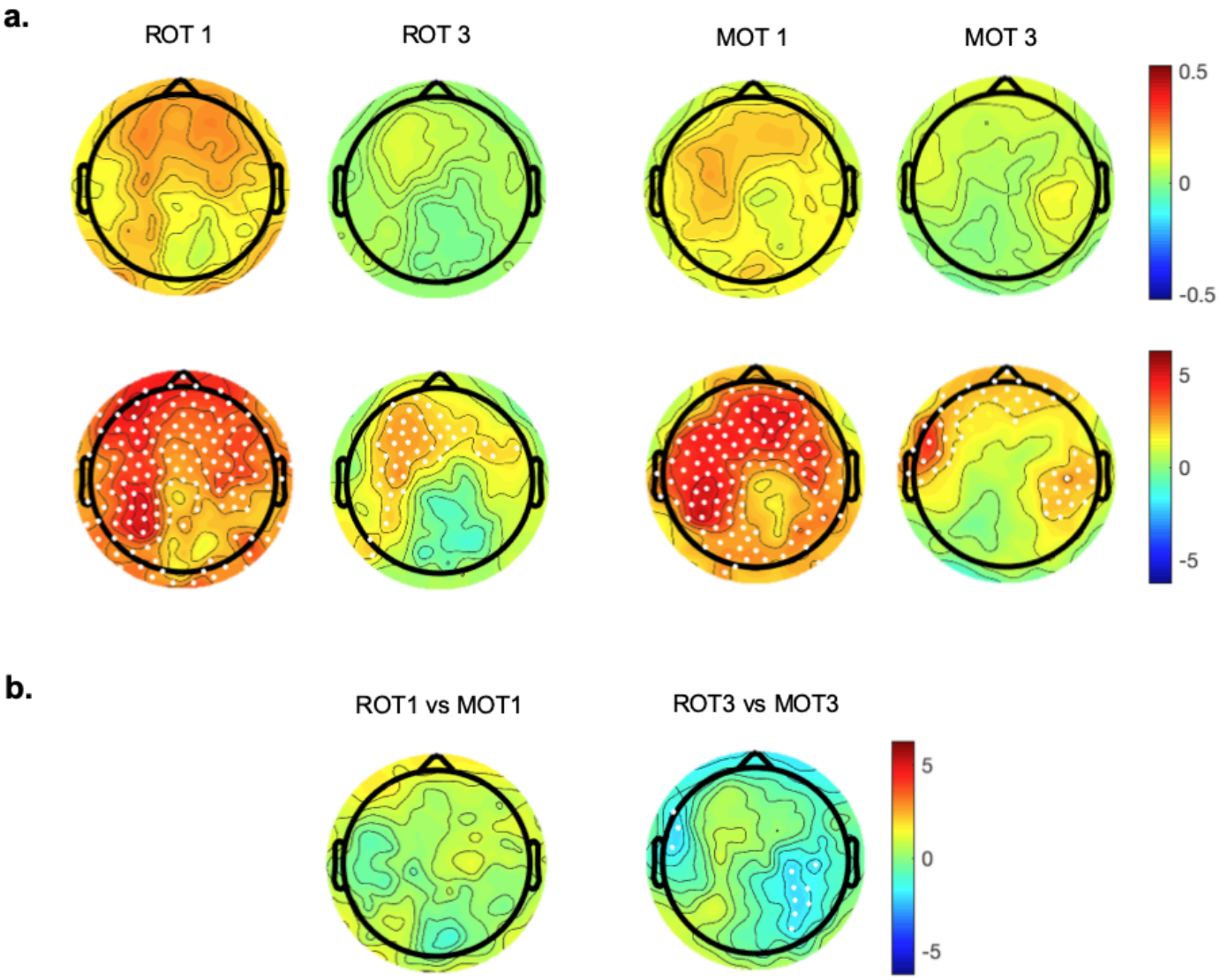


**Figure 1**

Within-block changes of average beta oscillatory activity in the ROT and MOT tasks. a. Top. Topographic distribution of the within-block changes -computed as the difference between the last and first two zero-degree rotation sets- in the first and last blocks of ROT (ROT1 and ROT3) and MOT (MOT1 and MOT3). Bottom. Bonferroni-corrected permutation t-values maps. Dots indicate significant electrodes ($p \leq 0.01$ for Block 1; $p \leq 0.05$ for Block 3). b. Maps of the Bonferroni-corrected permutation t-values comparing the within-block changes of the two tasks in the first block (ROT1 vs MOT1) and in the last block (ROT3 vs MOT3). Significant electrodes are reported as white dots.

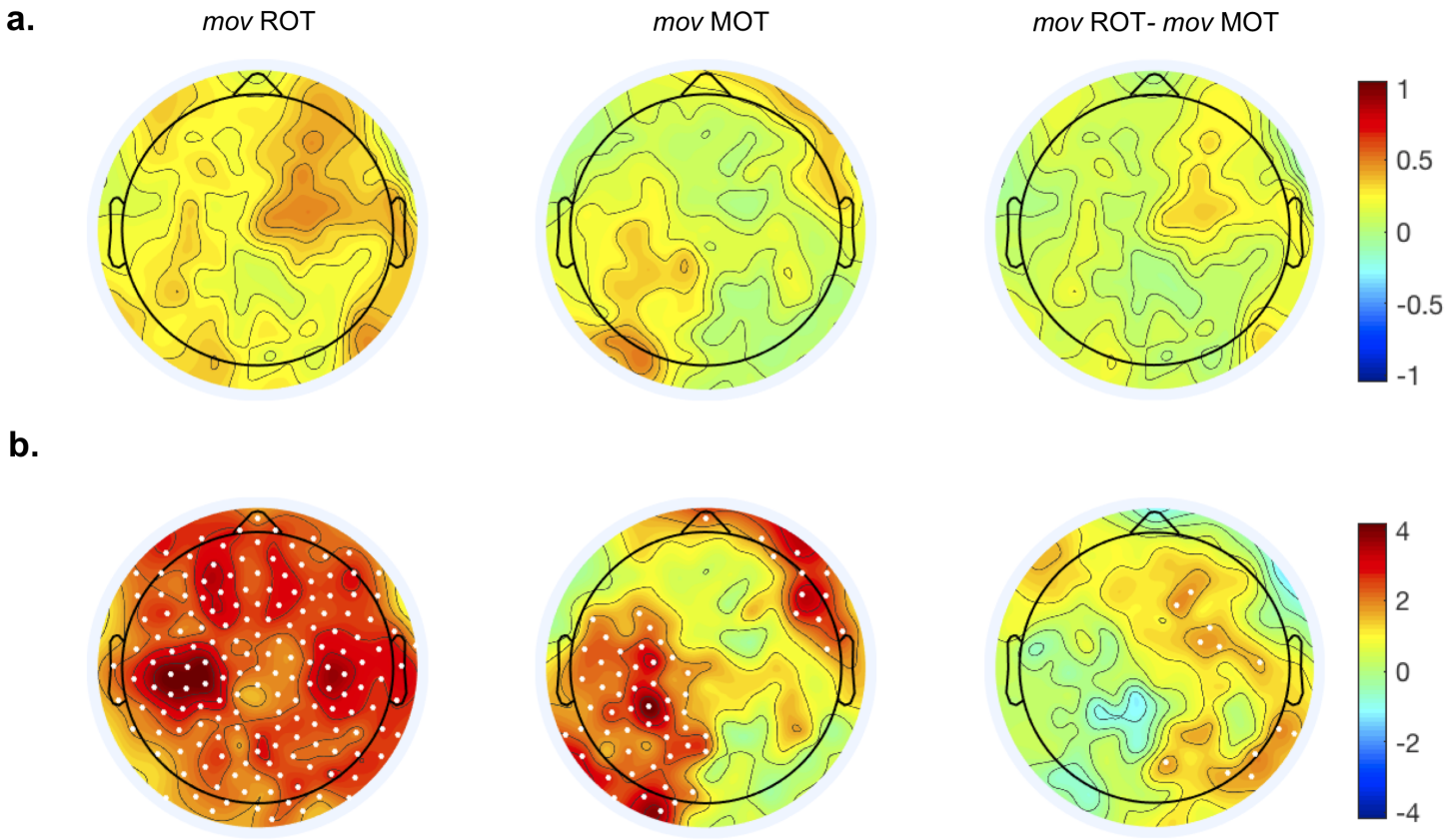


## Figure 2

Within-block changes of average beta oscillatory activity in mov. a. Topographic distribution of the between-block changes - computed as the difference between mov0 and mov3- in both ROTmov and MOTmov, and their differences (ROTmov vs MOTmov). b. Maps of the Bonferroni-corrected permutation t-values comparing the between-blocks changes in ROTmov, MOTmov and their relative difference. Significant electrodes are reported as white dots ($p \leq 0.05$).

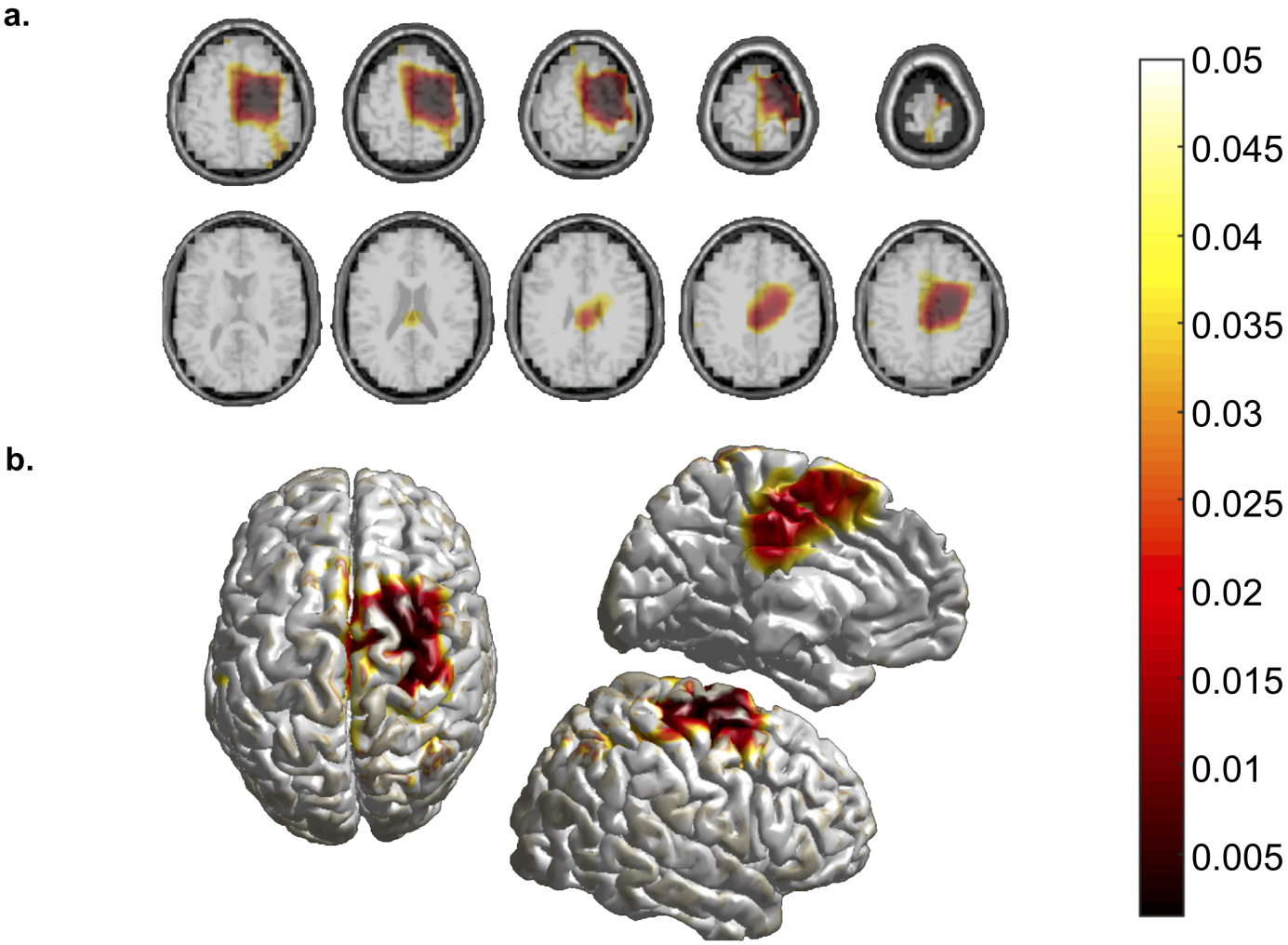


**Figure 3**

Bonferroni-corrected p-value distribution of Monte Carlo non-parametric permutation statistics on ROTmov and MOTmov source-reconstruction differences in between-blocks (mov3-mov0) post-movement beta activity increase. a. horizontal slices were obtained by interpolating the statistics onto the MRI template. b. surface plots were obtained by interpolation onto the MNI template.

## Supplementary Files

This is a list of supplementary files associated with this preprint. Click to download.

- SupplementalTableS1.docx
- SupplementalTableS2.docx